View metadata, citation and similar papers at core.ac.uk

brought to you by CORE

provided by Elsevier - Publisher Connector

Differential Geometry and its Applications 29 (2011) 329–347

Contents lists available at ScienceDirect

Differential Geometry and its Applications

www.elsevier.com/locate/difgeo

Boundary value problems on planar graphs and flat surfaces with integer cone singularities, II: The mixed Dirichlet–Neumann problem

Sa'ar Hersonsky

Department of Mathematics, University of Georgia, Athens, GA 30602, United States

ARTICLE INFO

Article history:
Received 1 September 2010
Available online 19 April 2011
Communicated by F. Pedit

MSC:
primary 53C43
secondary 57M50

Keywords:
Planar networks
Harmonic functions on graphs
Flat surfaces with conical singularities

ABSTRACT

In this paper we continue the study started in Hersonsky (in press) [16]. We consider a planar, bounded, m-connected region Ω, and let $\partial\Omega$ be its boundary. Let $\mathcal{T}$ be a cellular decomposition of $\Omega \cup \partial\Omega$, where each 2-cell is either a triangle or a quadrilateral. From these data and a conductance function we construct a canonical pair (S, f) where S is a special type of a (possibly immersed) genus $(m-1)$ *singular flat surface*, tiled by rectangles and f is an energy preserving mapping from $\mathcal{T}^{(1)}$ onto S. In Hersonsky (in press) [16] the solution of a Dirichlet problem defined on $\mathcal{T}^{(0)}$ was utilized, in this paper we employ the solution of a mixed Dirichlet–Neumann problem.

© 2011 Elsevier B.V. All rights reserved.

0. Introduction

Before stating our main result, we need to define a special kind of two-dimensional objects, *surfaces with propellors*. A flat, genus zero compact surface with $m > 2$ boundary components endowed with conical singularities, will be called *a ladder of singular pairs of pants*. A *sliced* Euclidean rectangle is a Euclidean rectangle in which two adjacent vertices are identified, and possibly a finite number of points on the opposite edge have been pinched.

Definition 0.1. A singular flat (possibly immersed), genus zero compact surface with $m > 2$ boundary components having conical singularities, will be called a surface with propellors, if it has a decomposition into the following pieces: a ladder of singular pairs of pants, sliced Euclidean rectangles, Euclidean rectangles and straight Euclidean cylinders.

We consider (as in [16]) a planar, bounded, m-connected region Ω, and let $\partial\Omega$ be its boundary. Let $\partial\Omega = E_1 \sqcup E_2$, where E_1 is the outermost component of $\partial\Omega$. Henceforth, we will let $\{\alpha_1, \ldots, \alpha_l\}$ be a collection of closed disjoint arcs contained in E_1, and let $\{\beta_1, \ldots, \beta_m\}$ be a collection of closed disjoint arcs contained in E_2. Let $\mathcal{T}$ be a cellular decomposition of $\Omega \cup \partial\Omega$, where each 2-cell is either a triangle or a quadrilateral. Invoke a *conductance function* on $\mathcal{T}^{(1)}$, making it a *finite network*, and use it to define a combinatorial Laplacian Δ on $\mathcal{T}^{(0)}$. These data will be called *Dirichlet–Neumann data* for $(\Omega, \partial\Omega, \mathcal{T})$. Let k be a positive constant, and let g be the solution of a mixed *Dirichlet–Neumann* boundary value problem (DN-BVP) defined on $\mathcal{T}^{(0)}$ and determined by requiring that

(1) $g|_{\alpha_i} = k$, for all $i = 1, \ldots, l$, and $g|_{\beta_j} = 0$, for all $j = 1, \ldots, m$,
(2) $\frac{\partial g}{\partial n}|_{(E_1 \setminus (\alpha_1 \cup \cdots \cup \alpha_l))} = \frac{\partial g}{\partial n}|_{(E_2 \setminus (\beta_1 \cup \cdots \cup \beta_m))} = 0$, for all $i = 1, \ldots, l$ and $j = 1, \ldots, m$,

E-mail address: saarh@math.uga.edu.
URL: http://www.math.uga.edu/~saarh.

0926-2245/$ – see front matter © 2011 Elsevier B.V. All rights reserved.
doi:10.1016/j.difgeo.2011.03.003

(3) $\Delta g = 0$ at every interior vertex of $\mathcal{T}^{(0)}$, i.e. g is *combinatorially harmonic*, and
(4) $\sum_{x\in\partial\Omega} \frac{\partial g}{\partial n}(\partial\Omega)(x) = 0$,

where (4) is a necessary consistent condition. Let $E(g)$ denote the *Dirichlet energy* of g. We may now state the main result of this paper:

Theorem 0.2 *(Main result). Let $(\Omega, \partial\Omega, \mathcal{T})$ be a bounded, m-connected, planar region endowed with a Dirichlet–Neumann data, with $m > 2$. Then there exists a surface with propellors $\mathcal{S}_\Omega$, and a mapping f which associates to each edge in $\mathcal{T}^{(1)}$ a unique Euclidean rectangle in S_Ω in such a way that the collection of these rectangles forms a tiling of S_Ω. Furthermore, f is boundary preserving, and f is energy preserving in the sense that $E(g) = \mathrm{Area}(S_\Omega)$.*

Throughout this paper a Euclidean rectangle will denote the image under an isometry of a planar Euclidean rectangle. For instance, some of the image rectangles that we will construct embed in a flat Euclidean cylinder. These cylinders will further be glued in a way that will not distort the Euclidean structure (see Sections 2 and 4 for the details).

In our setting, boundary preserving means that the rectangle associated to an edge $[u, v]$ in $\mathcal{T}^{(1)}$ with $u \in \partial\Omega$ has one of its edges on a corresponding boundary component of the surface. In the course of the proof of Theorem 0.2, it will become apparent that the number of singular points and their cone angles, the lengths of shortest geodesics between boundary curves in the ladder and the number of propellors, may be explicitly determined. In particular, the cone angles obtained by our construction are always integer multiples of $\pi/2$. Some classes of such surfaces are called *translation surfaces*, and for excellent accounts see for instance [18,21] and [24].

Also, the dimensions of each rectangle are determined by the given DN-BVP problem on $\mathcal{T}^{(0)}$. Concretely, for $[u, v] \in \mathcal{T}^{(1)}$, the associated rectangle will have its height equals to $(g(u) - g(v))$ and its width equals to $c(u, v)(g(u) - g(v))$, when $g(u) > g(v)$. Some of the rectangles are not embedded. We will comment on this point (which is also transparent in the proof of the theorem above) in Remark 5.12. In a snapshot, some of the rectangles which arise from intersection of edges with singular level curves of the DN-BVP solution are not embedded.

A *surface with dents and pillows* will denote the surface obtained by doubling a surface with propellors along its boundary. The following corollary is straightforward, thus establishing the statement in the abstract of this paper.

Corollary 0.3. *Under the assumptions of Theorem 0.2, there exists a canonical pair (S, f), where S is a flat surface with dents and pillows of genus $(m-1)$, having conical singularities and tiled by Euclidean rectangles. The mapping f is energy preserving from $\mathcal{T}^{(1)}$ into S, in the sense that $2E(g) = \mathrm{Area}(S)$.*

Proof. Given $(\Omega, \partial\Omega, \mathcal{T})$, glue together two copies of S_Ω (their existence is guaranteed by Theorem 0.2) along corresponding boundary components. This results in a flat surface $S = S_\Omega \bigcup_{\partial\Omega} S_\Omega$ of genus $(m-1)$ and a mapping $\bar{f}$ which restricts to f on each copy. □

The following two theorems are foundational and serve as building blocks in the proofs of the theorems above. In [16, Theorem 0.4] we proved the following:

Theorem 0.4 *(Discrete uniformization of an annulus [8]). Let $\mathcal{A}$ be an annulus and let $(\Omega, \partial\Omega, \mathcal{T}) = (\mathcal{A}, \partial\mathcal{A} = E_1 \sqcup E_2, \mathcal{T})$. Let $S_\mathcal{A}$ be a straight Euclidean cylinder with height $H = k$ and circumference*

$$C = \sum_{x\in E_1} \frac{\partial g}{\partial n}(x). \tag{0.5}$$

Then there exists a mapping f which associates to each edge in $\mathcal{T}^{(1)}$ a unique embedded Euclidean rectangle in $S_\mathcal{A}$ in such a way that the collection of these rectangles forms a tiling of $S_\mathcal{A}$. Furthermore, f is boundary preserving, and f is energy preserving in the sense that $E(g) = \mathrm{Area}(S_\mathcal{A})$.

A topological planar closed disk with four distinguished points on its boundary, its corners, will be called a quadrilateral. Let $\mathcal{R}$ be a quadrilateral endowed with a cellular decomposition. Let $\partial\mathcal{R} = \partial\mathcal{R}_{\mathrm{bottom}} \cup \partial\mathcal{R}_{\mathrm{left}} \cup \partial\mathcal{R}_{\mathrm{top}} \cup \partial\mathcal{R}_{\mathrm{right}}$ be a decomposition of $\partial\mathcal{R}$ into four non-trivial arcs of the cellular decomposition with disjoint interiors, in cyclic order. If the intersection of any two of these arcs is not empty, then it consists of a corner (all of which are vertices). A corner belongs to one and only one of the arcs. We solve a mixed Dirichlet–Neumann boundary value problem with $E_1 = E_2$, $\alpha_1 = \partial\mathcal{R}_{\mathrm{right}}$, $\beta_1 = \partial\mathcal{R}_{\mathrm{bottom}}$, $\beta_2 = \partial\mathcal{R}_{\mathrm{top}}$ (and hence that and $g|_{\partial\mathcal{R}_{\mathrm{left}}} = 0$). The second foundational theorem is proved in this paper:

Theorem 0.6 *(Discrete uniformization of a rectangle [8]). Let $\mathcal{R}$ be a quadrilateral. Let $S_\mathcal{R}$ be a Euclidean rectangle with width $W = k$ and height*

$$H = \sum_{x\in\partial\mathcal{R}_{\mathrm{right}}} \frac{\partial g}{\partial n}(\mathcal{R})(x). \tag{0.7}$$

Then there exists a mapping f which associates to each edge in $\mathcal{T}^{(1)}$ a unique embedded Euclidean rectangle in $S_{\mathcal{R}}$ in such a way that the collection of these rectangles forms a tiling of $S_{\mathcal{R}}$. Furthermore, f is boundary preserving, and f is energy preserving in the sense that $E(g) = \mathrm{Area}(S_{\mathcal{R}})$.

Given $(\Omega, \partial\Omega, \mathcal{T})$, we will work with the natural affine structure induced by the cellular decomposition. Let us denote this cell complex endowed with its affine structure by $\mathcal{C}(\Omega, \partial\Omega, \mathcal{T})$. Next, study the level curves of $\bar{g}$ on a 2-dimensional complex which is homotopically equivalent to $\mathcal{C}(\Omega, \partial\Omega, \mathcal{T})$, embedded in $\mathbb{R}^3$, obtained by using $\bar{g}$ as a height function on $(\Omega, \partial\Omega, \mathcal{T})$. We will work with the level curves of $\bar{g}$ or equivalently, with their projection on $\mathcal{C}(\Omega, \partial\Omega, \mathcal{T})$.

Once Theorem 0.6 is proved, we proceed to prove Theorem 0.2 as follows. We first construct a topological decomposition of Ω. Let $\{0, p_1, p_2, \ldots, p_{n-1}, k\}$ be the set of values of g at the singular vertices (see Definition 3.3) arranged in an increasing order. For $i = 0, \ldots, k$, consider the sub-domain of Ω defined by

$$\Omega_i = \left\{x \in \Omega \;\middle|\; p_i < g(x) < p_{i+1}\right\} \tag{0.8}$$

(where the value at x which is not a vertex is defined by the affine extension of g). In general Ω_i is multi-connected and (by definition) contains no singular vertices in its interior. Let $g_i = g|_{\Omega_i}$ be the restriction of g to $\Omega_i \cup \partial\Omega_i$. The definition of g_i involves (as in the proof of Theorem 0.6) new vertices (type I), and new edges and their conductance constants. In particular, each g_i is the solution of a D-BVP (Dirichlet boundary value problem) or a DN-BVP, on each one of the components of Ω_i.

By applying a topological–combinatorial index lemma (Lemma 3.7) and a splitting argument, we will conclude that Ω may be decomposed into a union (with disjoint interiors) of annuli, quadrilaterals or sliced quadrilaterals. We will finish the proof by showing that the gluing is geometric, i.e. that for all i, any part of $\partial\Omega_i$ has the same flux-gradient metric (Definition 1.6), with respect to the boundary value problems induced on each of the two components it belongs to.

Throughout this paper we will assume that the reader is familiar with the results and terminology of [16]. A theorem, two definitions and a process of modifying a boundary value problem that are essential to the applications of this paper, will be recalled in Section 1 in order to make this paper self contained. The rest of this paper is organized as follows. In Section 2 we prove Theorem 0.6. In Section 3 we prove a topological index lemma which is a generalization of [2, Theorem 1] and [20, Theorem 2]. This lemma may be regarded as a discrete version of the Hopf–Poincaré Index Theorem with additional terms arising from boundary data. In Section 4, we provide several other low complexity examples and their associated propelled surfaces. Some of these cases may be analyzed without using the topological lemma of Section 3; however, this lemma provides a uniform approach, hence we will apply it. Finally, Section 5 is devoted to the proof of Theorem 0.2.

Since one may view a Dirichlet boundary value problem as a special case of a Dirchlet–Neumann boundary problem, the main result in [16] follows from Theorem 0.2 of this paper. However, there is an essential difference between the methods of this paper and those in [16]. In some sense the construction of the image surfaces ($\mathcal{S}_\Omega$) in this paper is considerably less explicit than the construction in [16]. At this moment, we are unable to provide a structure theory for level curves of the DN-BVP. The structure theorem [16, Theorem 2.34] for level curves of D-BVP allowed us to cut the domain along the hierarchy of singular level curves until we obtain simple regions and then glue back. Thus, in this paper we are led to work with the subdomains Ω_i, which turns out to be sufficient for the applications of this paper. One may view our results and techniques in this paper as well as in [16], as providing purely combinatorial–topological analogues to classical counterparts. See in particular [1, Theorems 4–5], where a connection (in the smooth category) between *extremal length* of a family of curves and *Dirichlet Energy* of a boundary value problem is exploited.

Remark 0.9. The assertions of Theorem 0.6 may (in principle) be obtained by employing techniques introduced in the famous paper by Brooks, Smith, Stone and Tutte [8], in which they study square tilings of rectangles. They define a correspondence between square tilings of rectangles and planar multigraphs endowed with two poles, a source and a sink. They view the multigraph as a network of resistors in which current is flowing. In their correspondence, a vertex corresponds to a connected component of the union of the horizontal edges of the squares in the tiling; one edge appears between two such vertices for each square whose horizontal edges lie in the corresponding connected components. Their approach is based on *Kirckhhoff's circuit laws* that are widely used in the field of electrical engineering. We found the sketch of the proof of Theorem 0.4 given in [8] hard to follow. For a summary of other proofs of Theorem 0.6, a bit of the history of this problem, and generalizations, see Remark 0.5 in [16] (as well as [7,12,10,22], and [19]). We include our proof of Theorem 0.6, which is guided by similar principles to some of the ones mentioned above, yet significantly different in a few points, in order to make this paper self-contained. In addition, the important work of Bendito, Carmona and Encinas (see for example [4–6]) on boundary value problems on graphs allows us to use a unified framework to more general problems. Their work is essential to our applications and we have used parts of it quite frequently in [16], and this paper as well as its sequel [17].

1. A reminder

Finite networks. In this paragraph we will mostly be using the notation of Section 2 in [3]. Let $\Gamma = (V, E, c)$ be a planar *finite network*, that is a planar, simple, and finite connected graph with vertex set V and edge set E, where each edge $(x, y) \in E$ is assigned a *conductance* $c(x, y) = c(y, x) > 0$. Let $\mathcal{P}(V)$ denote the set of non-negative functions on V. Given $F \subset V$ we denote by F^c its complement in V. Set $\mathcal{P}(F) = \{u \in \mathcal{P}(V){:}\ S(u) \subset F\}$, where $S(u) = \{x \in V{:}\ u(x) \neq 0\}$. The set $\delta F = \{x \in F^c{:}\ (x, y) \in E \text{ for some } y \in F\}$ is called the *vertex boundary* of F. Let $\bar{F} = F \cup \delta F$ and let $\bar{E} = \{(x, y) \in E{:}\ x \in F\}$. Given $F \subset V$, let $\bar{\Gamma}(F) = (\bar{F}, \bar{E}, \bar{c})$ be the network such that $\bar{c}$ is the restriction of c to $\bar{E}$. We say that $x \sim y$ if $(x, y) \in \bar{E}$.

The following are discrete analogues of classical notions in continuous potential theory [14].

Definition 1.1. (See [4, Section 3].) Let $u \in \mathcal{P}(\bar{F})$. Then for $x \in \bar{F}$, the function $\Delta u(x) = \sum_{y \sim x} c(x, y)(u(x) - u(y))$ is called the Laplacian of u at x (if $x \in \delta(F)$ the neighbors of x are taken only from F) and the number

$$E(u) = \sum_{x \in \bar{F}} \Delta u(x) u(x) = \sum_{(x,y) \in \bar{E}} c(x, y)\big(u(x) - u(y)\big)^2, \tag{1.2}$$

is called the *Dirichlet energy* of u. A function $u \in \mathcal{P}(\bar{F})$ is called harmonic in $F \subset V$ if $\Delta u(x) = 0$, for all $x \in F$.

A fundamental property which we will often use is the *maximum–minimum principle*, asserting that if u is harmonic on $V' \subset V$, where V is a connected subset of vertices having a connected interior, then u attains its maximum and minimum on the boundary of V' (see [23, Theorem I.35]).

For $x \in \delta(F)$, let $\{y_1, y_2, \ldots, y_m\} \in F$ be its neighbors enumerated clockwise. The *normal derivative* (see [11]) of u at a point $x \in \delta F$ with respect to a set F is

$$\frac{\partial u}{\partial n}(F)(x) = \sum_{y \sim x,\, y \in F} c(x, y)\big(u(x) - u(y)\big). \tag{1.3}$$

The following proposition establishes a discrete version of the first classical *Green identity*. It plays a crucial role in the proofs of the main theorems in [15,16] and is essential to the applications of this paper as well as in its sequel [17].

Theorem 1.4. *(See [3, Prop. 3.1].) (The first Green identity.) Let $F \subset V$ and $u, v \in \mathcal{P}(\bar{F})$. Then we have that*

$$\sum_{(x,y) \in \bar{E}} c(x, y)\big(u(x) - u(y)\big)\big(v(x) - v(y)\big) = \sum_{x \in F} \Delta u(x) v(x) + \sum_{x \in \delta(F)} \frac{\partial u}{\partial n}(F)(x) v(x). \tag{1.5}$$

The flux-gradient metric. A *metric* on a finite network is a function $\rho : V \to [0, \infty)$. In particular, the length of a path is given by integrating ρ along the path (see [9] and [13] for a different definition). In [16, Definition 1.9] we defined a "metric" which will be used throughout this paper.

Definition 1.6. Let $F \subset V$ and let $f \in \mathcal{P}(\bar{F})$. The *flux-gradient metric* is defined by

$$\rho(x) = \frac{\partial f}{\partial n}(F)(x), \quad \text{if } x \in \delta(F). \tag{1.7}$$

This definition allows us to define a notion of length to any subset of the vertex boundary of F by declaring:

$$\text{Length}(\delta F) = \left| \sum_{x \in \delta F} \frac{\partial f}{\partial n}(F)(x) \right|. \tag{1.8}$$

In the applications of this paper, we will use the second part of the definition in order to define length of connected components of level curves of a boundary value solution. In [15, Definition 3.3], we defined a similar metric (l_2-gradient metric) proving several length-energy inequalities.

Simple modifications of a boundary value problem. We will often need to modify a given cellular decomposition as well as the boundary value problem associated with it. The need to do this is twofold. First, assume for example, that L is a fixed, simple, closed level curve. Since $L \cap \mathcal{T}^{(1)}$ is not (generically) a subset of $\mathcal{T}^{(0)}$, Definition 1.6 may not be directly employed to provide a notion of length to L. We therefore add vertices and edges according the following procedure. Such new vertices will be called vertices of type I.

Let $\mathcal{O}_1$, $\mathcal{O}_2$ be the two distinct connected components of L in Ω with L being the boundary of both (these properties follow by employing the Jordan curve theorem). We will call one of them, say $\mathcal{O}_1$, an *interior domain* if all the vertices which belong to it have g-values that are smaller than the g-value of L. The other domain will be called the *exterior domain*. Note that by the maximum principle, one of $\mathcal{O}_1$, $\mathcal{O}_2$ must have all of its vertices with g-values smaller than $g|_L$.

Let $e \in \mathcal{T}^{(1)}$ and $x = e \cap L$. For $x \notin \mathcal{T}^{(0)}$, we now have two new edges (x, v) and (u, x). We may assume that $v \in \mathcal{O}_1$ and $u \in \mathcal{O}_2$. We now define conductance constants $\tilde{c}(v, x)$ and $\tilde{c}(x, u)$ by

$$\tilde{c}(v, x) = \frac{c(v, u)(g(v) - g(u))}{g(v) - g(x)} \quad \text{and} \quad \tilde{c}(u, x) = \frac{c(v, u)(g(u) - g(v))}{g(u) - g(x)}. \tag{1.9}$$

By adding to $\mathcal{T}$ all the new vertices and edges, as well as the piecewise arcs of L determined by the new vertices, we obtain two cellular decompositions, $\mathcal{T}_{\mathcal{O}_1}$ of $\mathcal{O}_1$ and $\mathcal{T}_{\mathcal{O}_2}$ of $\mathcal{O}_2$. Also, two conductance functions are now defined on the one-skeleton of these cellular decompositions by modifying the conductance function for g according to Eq. (1.9) (i.e. changes are occurring only on new edges). One then follows the arguments preceding [16, Definition 2.7] and defines a modification of the given boundary value problem, the solution of which is easy to control (using the existence and uniqueness theorems in [3]). Second, it is easy to see that Theorem 1.4 may not be directly applied for a modified cellular decomposition and the modified boundary value problem defined on it. Informally, the modified graph of the network needs to have its boundary components separated enough, in terms of the combinatorial distance, in order for Theorem 1.4 to be applied. In order to circumscribe such cases, we will add enough new vertices along edges and change the conductance constants along new edges in the obvious way, i.e. the original solution will still be harmonic at each new vertex and will keep its values at the two vertices along the original edge. Such new vertices will called type II.

2. The case of a quadrilateral

We now describe the structure of the proof of Theorem 0.6. The proof consists of two parts. First, we will show that there is a well-defined mapping from $\mathcal{T}^{(1)}$ into a set of (Euclidean) rectangles embedded in the rectangle $S_{\mathcal{R}}$. The crux of this part is the fact that level curves of g have the same induced length (measured with the flux-gradient metric), and a simple application of the maximum principle. Second, we will show that the collection of these rectangles forms a tiling of $S_{\mathcal{R}}$ with no gaps. The dimensions of $S_{\mathcal{R}}$ and the first Green identity (Theorem 1.4) will allow us to end the proof by employing an energy-area computation.

Keeping the notation of the introduction, we let A, B, C, D be the corners of $\mathcal{R}$ ordered clockwise with A being the left lower corner and with $AB = \mathcal{R}_{\text{left}}$, $BC = \mathcal{R}_{\text{top}}$, $CD = \mathcal{R}_{\text{right}}$ and $DA = \mathcal{R}_{\text{bottom}}$ being the boundary arcs decomposition of $\partial\mathcal{R}$ (see Fig. 2.3).

Proposition 2.1. *For each $s \in [0, k]$, the associated g-level curve, l_s, is simple and parallel to AB, i.e. its endpoints lie on BC and DA, respectively, and it does not intersect $AB \cup CD$.*

Proof. Harmonicity of g implies that there exists a path in $\mathcal{T}^{(1)}$ from B to CD along which g is strictly increasing. Since g is extended linearly over $\mathcal{T}^{(1)}$, each value in $[0, k]$ is attained (perhaps at some point on an edge of this path). Let $s_0 \in [0, k]$ be any such value. The assertion of the proposition is certainly true for $s_0 = 0$ and for $s_0 = k$. Therefore assume that $s_0 \in (0, k)$ and that it is attained at some point which we will denote by v_0. By construction v_0 is not an endpoint for l_{s_0} unless $v_0 \in \partial\mathcal{R}$, and it is clear that $v_0 \notin AB \cup CD$. Extend l_{s_0} from v_0 through triangles and quadrilaterals to a line. It follows by the maximum principle that l_{s_0} is simple and it is not a circle. Also, the intersection of l_{s_0} with each 2-cell is a line segment whose intersection with the boundary of this cell consists of exactly two points, or a vertex. Since $\mathcal{T}^{(2)}$ is finite, l_{s_0} is a closed, connected interval, and by construction may have its endpoints only in $\partial\mathcal{R}$. Let P_{v_0} and Q_{v_0} be its endpoints. To finish the proof, we need to show that P_{v_0} and Q_{v_0} do not belong to the same boundary arc of $\partial\mathcal{R}$. It is clear that none of the endpoints can belong to $AB \cup CD$, so suppose (without loss of generality) that they belong to BC. Let $l = l(P_{v_0}, v_1, v_2, \ldots, Q_{v_0})$ be the path in BC connecting P_{v_0} to Q_{v_0}, and let $\mathcal{P}_{s_0}$ be the polygon formed by l_{s_0} and the arc l. Attach a copy of it, $\bar{\mathcal{P}}_{s_0}$, along l. The result is a polygonal disc $\mathcal{D}_{s_0}$ all of its boundary vertices having the same g-value, s_0.

Let $\bar{g}$ be the function which is defined on $\mathcal{D}_{s_0}$ by letting $\bar{g} = g$ on $\mathcal{D}_{s_0} \cap (\mathcal{R} \cup \partial\mathcal{R})$ and by letting $\bar{g}(\bar{v}) = g(v)$ for every $\bar{v}$ in the attached copy where $v \in \mathcal{P}_{s_0}$ is the combinatorial symmetric "reflection" of $\bar{v}$. By changing the conductance constants (only) along edges in l, the fact that g is harmonic in $\mathcal{R}$ and since

$$\frac{\partial g}{\partial n}(\mathcal{P}_{s_0})(v) = 0, \tag{2.2}$$

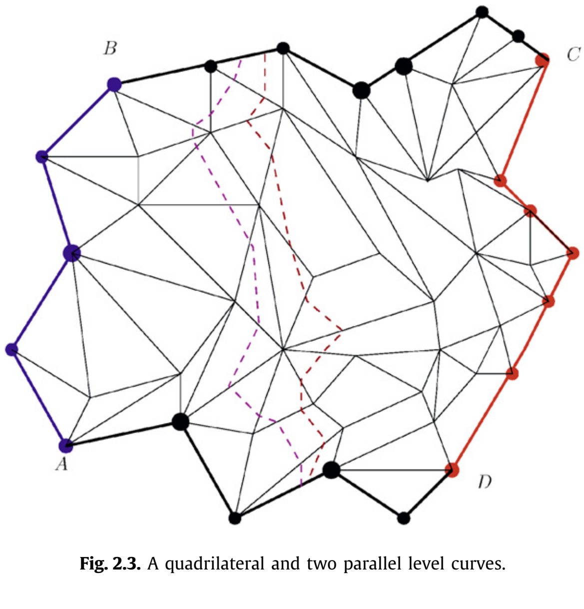

Fig. 2.3. A quadrilateral and two parallel level curves.

for every $v \in l$. It easily follows that $\bar{g}$ is harmonic in $\mathcal{D}_{s_0}$. However, $\bar{g}$ has constant boundary values, hence $\bar{g}$ must be a constant (by the maximum–minimum principle). This is absurd. □

Remark 2.4. Similarly, it follows by the harmonicity of g that for each $s \in [0, k]$, l_s is unique.

One useful consequence of Proposition 2.1 is that for each $s \in (0, k)$ the level curve l_s separates $\mathcal{R}$ into two quadrilaterals having disjoint interiors. The first has its left boundary equal to AB, its right boundary equal to l_s, its top boundary being the part of the top boundary of $\mathcal{R}$ connecting B to the endpoint of l_s on it, and its bottom boundary being part of the bottom boundary of $\mathcal{R}$ connecting A to the second endpoint of l_s. We will denote this quadrilateral by $\mathcal{O}_1$ and its complement in $\mathcal{R}$ by $\mathcal{O}_2$.

The length of a curve with respect to the flux-gradient metric (see Definition 1.8), which lies on the boundary of two regions, may be computed according to each one of them. The length will be said to be well-defined if it does not depend on the region chosen for carrying the computation.

Proposition 2.5. *For every $s \in [0, k]$, the length of its associated level curve l_s with respect to the flux-gradient metric, is well defined and is equal to*

$$H = \sum_{v \in CD} \frac{\partial g}{\partial n}(\mathcal{R})(v). \tag{2.6}$$

Furthermore, the following equality holds

$$\sum_{v \in CD} \frac{\partial g}{\partial n}(\mathcal{O}_2)(v) = -\sum_{v \in AB} \frac{\partial g}{\partial n}(\mathcal{O}_1)(v). \tag{2.7}$$

Proof. For $s = k$ the first assertion follows from the definition of the flux-gradient metric induced by g. Let s be any other value in $[0, k)$, and let l_s be its associated level curve. Let

$$\mathcal{V}_s = l_s \cap \mathcal{T}^{(1)}, \tag{2.8}$$

and define $\bar{g}$ at each point of the set $\mathcal{V}_s$ so that $\bar{g}(v) = g(v)$, for every $v \in \mathcal{T}^{(0)}$, and conductance constants on the added edges so that $\bar{g}$ is harmonic at each $v \in \mathcal{V}_s$, and

$$\frac{\partial \bar{g}}{\partial n}(\xi_1) = \frac{\partial \bar{g}}{\partial n}(\xi_2) = 0, \tag{2.9}$$

where ξ_1 and ξ_2 are the endpoints of l_s on BC and AD, respectively (the very last modifications are needed only if ξ_1 and ξ_2 are not in $\mathcal{T}^{(0)}$). Note that the set $\mathcal{V}_s$ comprises (generically) vertices of type I (see the last paragraph in Section 1).

We now apply Green's Theorem (Theorem 1.4) with $u = \bar{g}$ and $v \equiv 1$ over the quadrilateral $\mathcal{O}_2$, which is determined by l_s, $\xi_1 C$, CD and $D\xi_2$ to obtain

$$0 = \sum_{t \in l_s} \frac{\partial \bar{g}}{\partial n}(\mathcal{O}_2)(t) + \sum_{p \in CD} \frac{\partial \bar{g}}{\partial n}(\mathcal{O}_2)(p), \tag{2.10}$$

and hence that

$$\left|\sum_{t \in l_s} \frac{\partial \bar{g}}{\partial n}(\mathcal{O}_2)(t)\right| = \left|\sum_{p \in CD} \frac{\partial g}{\partial n}(\mathcal{O}_2)(p)\right| = \sum_{p \in CD} \frac{\partial g}{\partial n}(\mathcal{O}_1)(p) = \sum_{p \in CD} \frac{\partial g}{\partial n}(\mathcal{R})(p), \tag{2.11}$$

which completes the proof of the first assertion. Note that in order to apply Green's Theorem we may need to add vertices of type II and change the conductance constants along added edges (see the last paragraph in Section 1).

By applying Green's Theorem (Theorem 1.4) to $\mathcal{R}$ one obtains the second assertion (as is the case with the last equality in Eq. (2.11), both sides of the equation have the same value when computed relative to $\mathcal{R}$). In particular, this means that the computation of the length of l_s with respect to the flux-gradient metric does not depend on which one of the two quadrilaterals, $\mathcal{O}_1$ or $\mathcal{O}_2$, it is carried. □

Given a Euclidean rectangle $Q = [0, W] \times [0, H]$ embedded in the Euclidean plane, we will endow it with the naturally induced coordinates. Its boundary components $[0, W] \times \{0\}$, $\{0\} \times [0, H]$, $[0, W] \times \{H\}$ and $\{W\} \times [0, H]$ will be called *bottom*, *left*, *top* and *right*, respectively. Before providing the proof of Theorem 0.6, we need a definition which will simplify keeping track of the mapping f.

Definition 2.12. A marker on a Euclidean rectangle is a horizontal closed interval which is the isometric image of $[a, b] \times \{t\}$, for some $t \in [0, H]$ and $[a, b] \subset [0, W]$ with $a < b$. The marker's leftmost end-point corresponds to (a, t) and its rightmost end-point to (b, t).

Proof of Theorem 0.6. Let $S_{\mathcal{R}}$ be a straight Euclidean rectangle with width $W = k$ and height

$$H = \sum_{x \in \partial \mathcal{R}_{\text{right}}} \frac{\partial g}{\partial n}(\mathcal{R})(x). \tag{2.13}$$

Let $\mathcal{L} = \{L_1, \ldots, L_k\}$ be the level sets of g corresponding to the vertices in $\mathcal{T}^{(0)}$ arranged in descending g-values order. We add a vertex at each intersection of an edge with an L_i, $i = 1, \ldots, k$ (which is not already a vertex in $\mathcal{T}^{(0)}$), and if necessary more vertices on edges so that any two successive level curves in $\mathcal{L}$ are at combinatorial distance (at least) two. As before, the first group of added vertices is of type I and the second is of type II.

Starting with $x_1 = C$, we order the vertices $\{x_1 = C, \ldots, x_p = D\}$ in L_1 $(= CD)$, as well as the vertices on any other level curve, in a monotone decreasing order. Let $\{y_1, y_2, \ldots, y_t\}$ be the type I neighbors of x_1 in the new cellular decomposition oriented counterclockwise (which will henceforth be assumed to be the ordering of the neighbors of any vertex). We identify x_1 with (k, H) in the coordinates mentioned above, and associate markers $\{m_{x_1,y_1}, \ldots, m_{x_1,y_t}\}$ with x_1 in the following way. For $s = 1, \ldots, t$, the length of the marker m_{x_1,y_s} is equal to (the constant) $g(x_1) - g(y_s)$ and its rightmost end-point is positioned on the right boundary of $S_{\mathcal{A}}$ at height

$$H - \sum_{k=1}^{s-1} c(x_1, y_k)\bigl(g(x_1) - g(y_k)\bigr). \tag{2.14}$$

For each edge $e_{u,v} = [u, v]$ with $g(u) > g(v)$, let $Q_{u,v}$ be a Euclidean rectangle with width equal to $g(u) - g(v)$ and height equal to $c(u, v)(g(u) - g(v))$. We will identify a Euclidean rectangle and its image under an isometry. For $s = 1, \ldots, t$, we position Q_{x_1,y_s} in $S_{\mathcal{A}}$ in such a way that its top boundary edge coincides with m_{x_1,y_s}. By construction and the position of the markers,

$$Q_{x_1,y_s} \cap Q_{x_1,y_{s+1}} = m_{x_1,y_{s+1}}. \tag{2.15}$$

Assume that we have placed markers and rectangles associated to all the vertices up to x_k where $k < p$; let z_1 be the uppermost neighbor of x_{k+1} and let $Q_{x_k,v}$ be the lowermost rectangle associated with x_k (see Fig. 2.16). That is, v is the lowermost vertex which is a neighbor of x_k (it may of course happen that $v = z_1$). We now position the marker m_{x_{k+1},z_1} so that it is lined with the bottom boundary edge of $Q_{x_k,v}$, and its rightmost end-point is on the right boundary of $S_{\mathcal{A}}$ at height which is given by the obvious modification of Eq. (2.14). We continue placing markers and rectangles corresponding to the rest of the neighbors of x_{k+1}, and terminate these steps when $k = p$. Note that the right boundary of $S_{\mathcal{A}}$ is completely covered by the right boundary edges of the rectangles constructed above, where intersections between any two of these edges is either a vertex or empty.

For all $1 < n < k$, assume that all the markers corresponding to vertices in L_{n-1} and their associated rectangles have been placed as above in such a way that the following conditions, which we call *consistent*, hold. For $[w, v] \in T^{(1)}$ with $g(w) > g(v)$ and $s \in [w, v]$ a vertex of type I, the rightmost end-point of the marker $m_{s,v}$ coincides with the leftmost end-point of the marker $m_{w,s}$; moreover, the union of the rectangles $Q_{w,s}$, $Q_{s,v}$ tile $Q_{v,w}$. Informally, if these conditions are met, this will allow us to "continuously extend" rectangles associated with edges that cross level curves along these curves, and therefore will show that edges in $\mathcal{T}^{(1)}$ are mapped in one to one fashion (perhaps in several steps) onto a unique rectangle, $Q_{w,v}$.

We will now describe how to place the markers and rectangles corresponding to the vertices of the level set L_n, for $n > 2$. The rightmost end-point of each marker associated with a vertex $v \in L_n$ and any of its neighbors in L_{n+1} is placed

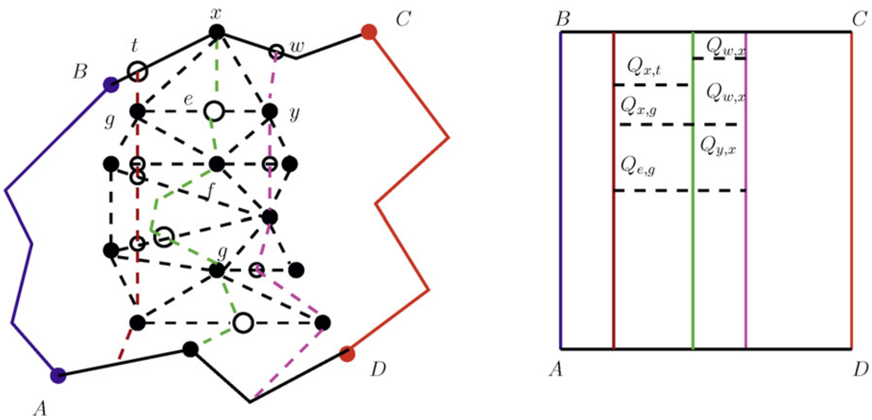

Fig. 2.16. Several rectangles in $S_{\mathcal{R}}$ after the completion of the construction.

in $S_{\mathcal{R}}$ on the vertical line corresponding to $g(v)$ (the actual height on this level curve is computed by a formula which is an easy modification of Eq. (2.14)). Observe that v is a vertex in some $[q_i, v]$, where q_i belongs to L_{n-1}. Choose among all such edges the uppermost (viewed from $v \in L_n$). Let $[q_0, v]$ be this edge and let $m_{q_0,v}$ be its marker. Place $m_{v,w}$, the marker of v which corresponds to an edge $[v, w]$, with w being the uppermost vertex among the neighbors of v in L_{n+1}, so that its rightmost end-point coincides with the leftmost end-point of $m_{q_0,v}$. To conclude the construction, continue as above, exhausting all the markers emanating from v, and vertices in L_n.

By the maximum principle, our construction, and the fact that all level curves have their lengths (with respect to the flux-gradient metric) equal to H, it is clear that the union of the rectangles is contained in $S_{\mathcal{R}}$.

Proposition 2.17. *The placement of rectangles associated to the construction of markers as described above is consistent.*

Proof. We prove the assertion by induction on the set of level curves. The assertion is obviously true for all rectangles associated with markers emanating from L_1, since no such marker is a continuation of another one. Let s_0 be a vertex of type I on L_n, $n > 2$. By definition, s_0 is connected to a unique vertex $v_0 \in L_{n+1}$ and to a unique vertex $w_0 \in L_{n-1}$. We first consider the case in which s_0 is the only type I vertex on L_n. It is easy to check that the following system of equations with the two unknowns $\tilde{c}(w_0, s_0)$ and $\tilde{c}(s_0, v_0)$ has a non-trivial solution

$$\begin{aligned}&\tilde{c}(w_0, s_0)\big(g(w_0) - g(s_0)\big) = \tilde{c}(s_0, v_0)\big(g(s_0) - g(v_0)\big), \quad \text{and}\\&\tilde{c}(w_0, s_0)\big(g(w_0) - g(s_0)\big) = c(w_0, v_0)\big(g(w_0) - g(v_0)\big).\end{aligned} \tag{2.18}$$

The unknowns present the conductance constants to be assigned to $[w_0, s_0]$ and $[s_0, v_0]$, respectively, so that the modified DN-BVP solution function $\bar{g}$ is harmonic at s_0. By the construction of the rectangles, this implies that the height of Q_{s_0,v_0} is the same as the height of $Q(w_0, s_0)$, so that they can be glued along the appropriate edges. The second equation reflects that the height of the rectangles associated to m_{w_0,s_0} and m_{s_0,v_0} is equal to the height of the rectangle which one would associate to m_{w_0,v_0} (in the case that there were no type I vertices on $[w_0, v_0]$). In other words, the construction of rectangles is consistent and once an edge is split by a type I vertex, the two constructed rectangles may be glued along the appropriate edges; thus we obtain the same effect as constructing the rectangle associated to the original edge. Note that since $g(w_0) - g(v_0) = (g(w_0) - g(s_0)) + (g(s_0) - g(v_0))$, matching the widths of the above rectangles is not an issue.

Assume now that s_q is the first vertex of type I in L_n which is lower than s_0. By definition, s_q is connected to a unique vertex w_p in L_{n-1} and to a unique vertex $v_l \in L_{n+1}$. Let $\{s_1, \ldots, s_{q-1}\}$ be the vertices in L_n between s_0 and s_q, and let $\{w_1, \ldots, w_{p-1}\}$ be the vertices in L_{n-1} between w_0 and w_p. Let $\mathcal{Q}_1 = \mathcal{Q}_{w_0,s_0,s_q,w_p}$ be the quadrilateral enclosed by $[w_0, s_0] \cup [w_p, s_q] \cup L_{n-1} \cup L_n$, and which contains $\{w_0, \ldots, w_p\}$, and let $\mathcal{Q}_2 = \mathcal{Q}_{s_0,v_0,s_q,v_l}$ be the quadrilateral enclosed by $[s_0, v_0] \cup [s_q, v_l] \cup L_n \cup L_{n+1}$, and which contains $\{s_0, \ldots, s_q\}$ (see Fig. 2.19).

In order to prove that the consistent conditions hold for all markers and rectangles created in this step, it suffices to prove it at s_q; assuming (without loss of generality) that the first marker associated with vertices in L_n, that was placed in a consistent way, is m_{s_0,v_0}. By the construction of the markers (see in particular Eq. (2.14) suitably adapted) we need to prove that

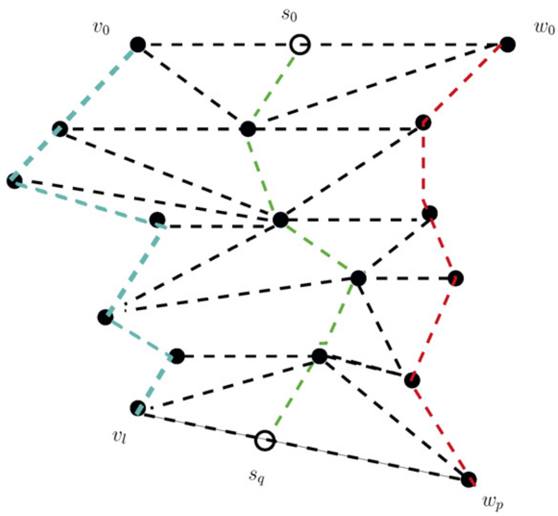

Fig. 2.19. Viewing $Q_1 \cup Q_2$.

$$\sum_{i=1}^{p-1} \frac{\partial \bar{g}}{\partial n}(\mathcal{Q}_1)(w_i) + \frac{\partial \bar{g}}{\partial n}(\mathcal{Q}_1)_{\text{low-left}}(w_0) + \frac{\partial \bar{g}}{\partial n}(\mathcal{Q}_1)_{\text{top-left}}(w_p)$$
$$= \sum_{i=1}^{q-1} \frac{\partial \bar{g}}{\partial n}(\mathcal{Q}_2)(s_i) + \frac{\partial \bar{g}}{\partial n}(\mathcal{Q}_2)_{\text{low-left}}(s_0) + \frac{\partial \bar{g}}{\partial n}(\mathcal{Q}_2)_{\text{top-left}}(s_q), \tag{2.20}$$

where the subscripts "low-left" and "top-left" are posted to emphasize that neighbors in the expressions are taken from $\mathcal{Q}_1$ or $\mathcal{Q}_2$ only. It is easy to check that since $\bar{g}$ is harmonic at each s_i, $i = 0, \dots, q$ (as well as elsewhere), and since s_0 and s_q are type I vertices, Eq. (2.20) holds.

We will now finish the proof by showing that the collection of rectangles constructed above tiles $S_{\mathcal{R}}$ leaves no gaps. Without loss of generality, suppose that the collection of the rectangles described above does not cover a strip of the form $[t_1, t_2] \times [h_0, h_1]$ in $S_{\mathcal{R}}$, where $0 \leqslant t_1 < t_2 \leqslant k$ and $0 \leqslant h_0 < h_1 \leqslant H$. Since g is harmonic there exists at least one path whose vertices belong to $\mathcal{T}^{(0)}$ such that the values of g along this path are strictly decreasing from k to 0. In particular, the value t_2 is attained at some interior point of an edge or at some vertex of this path. By construction, a gap in a g-level curve (i.e. an arc of a level curve which is not covered by the left edges of rectangles) never occurs when t_2 is the g-value associated to a vertex in the modified cellular decomposition, $\tilde{\mathcal{T}}$.

Hence, we may assume that t_2 is attained in the interior of an edge. Let L_{t_2} be the corresponding level curve. Recall that L_{t_2} is simple and parallel to CD with its two endpoints belonging to AD and BC, respectively (as is the case with all other level curves of g; see Proposition 2.1). We now follow the construction at the beginning of the proof, and let $\{u_1, u_2, \dots, u_q\}$ be all the new vertices on L_{t_2}, that is, we place a vertex at each intersection of an edge in $\tilde{\mathcal{T}}^{(1)}$ with L_{t_2}. By Proposition 2.6 the length of L_{t_2} (with respect to the flux-gradient metric) is equal to H. Moreover, this length is equal to

$$\sum_{i=1}^{q} \frac{\partial g}{\partial n}(\mathcal{O}_1)(u_i), \tag{2.21}$$

where $\mathcal{O}_1$ is the interior of the rectangle enclosed by AB (part of) BC, L_{t_2} and (part of) DA (see the end of the proof of Proposition 2.5). In particular, in principle we may now place in a consistent way, markers and rectangles associated to the collection of edges emanating from the vertices $\{u_1, u_2, \dots, u_q\}$ so that L_{t_2} is completely covered by the left edges of these rectangles. Since g is extended affinely over edges, every value between h_0 and h_1 is attained by g. Repeating this argument shows that all level curves are covered by rectangles. Hence the collection of rectangles leaves no gaps in $S_{\mathcal{A}}$.

Using an area argument, we now finish the proof by showing that there is no overlap between any two of the rectangles. Let $\mathcal{U}$ be the union of all the constructed rectangles. By definition,

$$\text{Area}(\mathcal{U}) = \sum_{[x,y] \in \tilde{\mathcal{T}}^{(1)}} c(x, y)\big(g(x) - g(y)\big)\big(g(x) - g(y)\big). \tag{2.22}$$

Note that the sum appearing in the right-hand side of Eq. (2.22) is computed over $\tilde{\mathcal{T}}^{(1)}$, the induced cellular decomposition. A simple computation (using Eq. (2.20)) and the fact that the construction is consistent shows that this sum is equal to the one taken over all $[x, y] \in \mathcal{T}^{(1)}$. Hence, the right-hand side of this equation is the energy $E(g)$ of g (see Definition 1.1). Therefore, by the first Green identity, applied with $u = v = g$ (see Theorem 1.4), the boundary conditions imposed on g, and the dimensions of $S_{\mathcal{R}}$, we have

$$E(g) = \text{Area}(\mathcal{U}) = \text{Area}(S_{\mathcal{R}}). \tag{2.23}$$

Hence, since the union of the rectangles do not leave gaps, and are all contained in $S_{\mathcal{R}}$, they must tile $S_{\mathcal{R}}$. It is also evident that the mapping f constructed is energy preserving. □

Remark 2.24. In the forthcoming applications and examples of this paper, we will often need to use a slight generalization of Theorem 0.6. First, we will need to allow the domain to be sliced. That is, a quadrilateral, two of his adjacent vertices that belong to the left boundary (or right boundary), are identified, and possibly a finite number of points on the right boundary (or left boundary) are also identified (not necessarily to the same point). See the next section and in particular Example 4.13.

One considers a sliced quadrilateral as a quotient of a quadrilateral in the obvious way. The construction of Theorem 0.6 goes through with the image being a Euclidean rectangle under the appropriate quotient. Note that some of the image rectangles are not going to be embedded. However, the embedding fails in a mild way. For a similar situation in the case of a planar pair of pants, and corresponding analysis for higher genus cases in the setting of D-BVP, see [15, Section 4].

3. An index lemma

Let $\mathcal{G}$ be a polyhedral surface with (possible empty) boundary $\partial\mathcal{G}$. Let $f : \mathcal{G}^{(0)} \to \mathbb{R}^+ \cup \{0\}$ be a function such that any two adjacent vertices are given different values. Let $v \in \mathcal{G}^{(0)}$ with $v \notin \partial\mathcal{G}$, and let $w_1, w_2, \dots, w_k$ be its k neighbors enumerated counterclockwise. Following [20, Section 3], consider the number of sign changes in the sequence $\{f(w_1)-f(v), f(w_2)-f(v), \ldots, f(w_k)-f(v), f(w_1)-f(v)\}$, which we will denote by $\mathrm{Sgc}_f(v)$. The index of $v \in \mathcal{G}$ is defined as

$$\mathrm{Ind}_f(v) = 1 - \frac{\mathrm{Sgc}_f(v)}{2}. \tag{3.1}$$

For the applications of this paper we need to consider the situation in which $\partial\mathcal{G} \neq \emptyset$. Let $\bar{v} \in \partial\mathcal{G}$ and let $q_1, q_2, \ldots, q_l$ be its neighbors in $\mathcal{G}$ enumerated counterclockwise. Consider the number of sign changes in the sequence $\{f(q_1)-f(\bar{v}), f(q_2)-f(\bar{v}), \ldots, f(q_l)-f(\bar{v})\}$, which we will keep denoting by $\mathrm{Sgc}_f(\bar{v})$. The index of $\bar{v} \in \partial\mathcal{G}$ is defined as

$$\mathrm{Ind}_f(\bar{v}) = \frac{1}{2}\left(1 - \frac{2\,\mathrm{Sgc}_f(\bar{v})}{2}\right). \tag{3.2}$$

Definition 3.3. A vertex whose index is different from zero will be called singular; otherwise the vertex is regular. A level set which contains at least one singular vertex will be called singular; otherwise the level set will be called regular.

A nice connection between the combinatorics and the topology is provided by the following theorem, which may be considered as a discrete Hopf–Poincaré Theorem.

Theorem 3.4. *(See [2, Theorem 1], [20, Theorem 2].) (An index formula.) Suppose that $\mathcal{G}$ is closed, then we have*

$$\sum_{v \in \mathcal{G}} \mathrm{Ind}_f(v) = \chi(\mathcal{G}). \tag{3.5}$$

Remark 3.6. Note that due to the topological invariance of $\chi(\mathcal{G})$ once the equation above is proved for a triangulated polyhedron, it holds (keeping the same definitions for $\mathrm{Sgc}_f(\cdot)$ and $\mathrm{Ind}_f(\cdot)$ as well as the assumption on f) for any cellular decomposition of $\chi(\mathcal{G})$. Also, while the theorem above is stated and proved for a closed polyhedral surface, it is easy to show that it holds in the case of a surface with boundary, where there are no singular vertices on the boundary (simply by doubling along the boundary).

We now prove a generalization of Theorem 3.4 which includes the case of singular vertices on the boundary as well as the case in which f admits constant values on some arcs of the boundary. Some immediate applications of our generalization will be provided in Sections 4 and 5 providing the control we need on the number of critical points as well as their indices.

Lemma 3.7. *Let Ω be a bounded, planar, n-connected domain with $\partial\Omega$ as its boundary. Suppose that $\Omega \cup \partial\Omega$ is endowed with a cellular decomposition, denoted by $\mathcal{T}$, in which each 2-cell is a triangle or a quadrilateral. Suppose that l closed and disjoint arcs are specified on the outer boundary of $\partial\Omega$, and that m closed and disjoint arcs are specified on the other boundary components of $\partial\Omega$.*

Let $f : \mathcal{T}^{(0)} \to \mathbb{R}^+ \cup \{0\}$ be a function which satisfies the following:

(1) $\max(f)$ *is attained exactly at each vertex in $\mathcal{T}^{(0)}$ which lies on any of the l arcs,*
(2) $\min(f)$ *is attained exactly at each vertex in $\mathcal{T}^{(0)}$ which lies on any of the m arcs, and*
(3) *any two adjacent vertices in $\mathcal{T}^{(0)}$, other than the ones in* (1) *and* (2) *have different f-values.*

Then we have

$$\sum_{v \in \Omega} \mathrm{Ind}_f(v) + \sum_{\bar{v} \in \partial\Omega} \mathrm{Ind}_f(\bar{v}) + \frac{l+m}{2} = \chi(\Omega). \tag{3.8}$$

Proof. We first collapse each one of the arcs in $\partial\Omega$ on which f attains a maximum or a minimum value to a single vertex. The resulting planar domain Ω' is bounded and n-connected. The cellular decomposition $\mathcal{T}$ is changed to a new one $\mathcal{T}'$ in the following way. Any triangle in $\mathcal{T}^{(2)}$ with two of its vertices having the same f value is turned into a digon. Every quadrilateral with two of its vertices having the same f values is turned into a triangle. These changes occur (if at all) only at combinatorial distance which is equal to one from the arcs on which f attains a constant value. We now collapse all digons and multi-gons connecting two vertices (one of which is on $\partial\Omega'$) to a single edge connecting these vertices. In particular, we have that $\chi(\Omega) = \chi(\Omega')$, and $\mathcal{T}'$ is comprised of triangles and quadrilaterals. Furthermore, f attains its maximum on exactly l vertices in the outer boundary of $\partial\Omega'$ and its minimum on exactly m vertices in the inner boundary of $\partial\Omega'$. Also, any two adjacent vertices in $\mathcal{T}'^{(0)}$ have different f-values. The indices and the number of the singular interior vertices as well as the indices and the number of singular vertices that are on $\partial\Omega'$ and are not (global) maximum or minimum vertices has not changed.

We now double Ω' along its boundary $\partial\Omega'$ and obtain a closed polyhedral surface $\mathcal{G}$ of genus $\chi(\mathcal{G}) = 2\chi(\Omega')$. The index of each interior singular vertex is not changed; however, their number is doubled. Let $\bar{v} \in \mathcal{T}'^{(0)} \cap \partial\Omega'$ be a singular vertex, and denote by $\bar{v}^0$ this vertex in the double of Ω'. Note that

$$\mathrm{Sgc}_f(\bar{v}^0) = 2\,\mathrm{Sgc}_f(\bar{v}), \tag{3.9}$$

and therefore,

$$\mathrm{ind}_f(\bar{v}^0) = 2\,\mathrm{ind}_f(\bar{v}). \tag{3.10}$$

That is, the index of any boundary singular vertex which is not a maximum or a minimum is doubled; however, the number of such vertices is not changed. In the double, we also have exactly l vertices on which f attains its maximum, and exactly m vertices on which f attains its minimum. It is easy to check that

$$\mathrm{Ind}_f(\bar{v}^0) = 1, \tag{3.11}$$

whenever v is a maximum or a minimum vertex. Hence, by applying Theorem 3.4 to $\mathcal{G}$ we obtain the following equation.

$$2\sum_{v\in\Omega} \mathrm{Ind}_f(v) + \sum_{\bar{v}\in\partial\Omega} 2\,\mathrm{Ind}_f(\bar{v}) + (l+m) = \chi(\mathcal{G}) = 2\chi(\Omega). \tag{3.12}$$

The assertion of the theorem follows immediately. Let t be the total number of endpoints of the arcs on which f is constant. Since $\frac{l+m}{2} = \frac{t}{4}$ we will often use an equivalent formulation of Eq. (3.12). □

4. A few low complexity examples and their surfaces with propellors

In this section we will employ the index lemma (Lemma 3.7) and study a few low complexity examples. While it is possible to analyze some of the examples in this section without applying the index lemma, its usage considerably simplifies the analysis. These examples pave the way for the understanding of the general case which will be discussed in the next section.

Example 4.1 *(A quadrilateral with two boundary arcs on which f is constant).* This example was studied in length in Section 2. However, it is worth noting that in this case $l = m = 1$ and $t = 4$. Hence, the right-hand side of Eq. (3.12) minus $t/4$ is equal to zero. Since the index of an interior singular vertex is smaller or equal to -1, and the index of a singular boundary vertex is smaller or equal to $-\frac{1}{2}$, it follows that in this case, there are no singular vertices. This conclusion is consistent with the assertion of Proposition 2.1.

Example 4.2 *(An annulus with one outer Neumann arc).* Let $\mathcal{A}$ be a planar annulus with boundary $\partial\mathcal{A} = E_1 \cup E_2$, where E_1 is the outer boundary. Let α_1 be a closed arc in E_1 with endpoints Q and P (see Figs. 4.6 and 4.7). We solve the DN-BVP as described in the introduction. In particular, we have $l = 1$ and $t = 2$, and hence that the right-hand side of Eq. (3.12) minus $t/4$ is equal to $-\frac{1}{2}$. Therefore, the only possibility is that there exists only one singular boundary vertex which must belong to $E_1 \setminus \alpha_1$. We will denote this vertex by u_s, and its associated level curve by l_s. Since the index of u_s is equal to $-\frac{1}{2}$, there must be at least two arcs of l_s which pass through u_s. It follows by the maximum principle that there are exactly two arcs, and that l_s is simple. Moreover, $E_2 \cup l_s$ comprises the boundary of an annulus which we will denote by $\mathcal{A}_{l_s,E_2}$. It follows that $\mathcal{A}$ is topologically the union (along l_s) of a topological quadrilateral in which two adjacent vertices have been identified and an annulus. Such a quadrilateral will henceforth be called a *sliced quadrilateral*. The following lemma will show that this decomposition is geometric.

Let $\mathcal{V} = \{u_s, v_1, v_2, \ldots, v_k\} \in l_s$ be the set of vertices enumerated counterclockwise. Recall that some of these vertices are created due to the intersections of edges in $\mathcal{T}^{(1)}$ with l_s (type I), while others may belong to $\mathcal{T}^{(0)}$. For any type I vertex, we define the conductance along the two new edges it induces according to Eq. (2.20). In particular, if we let $\bar{g}$ denote the solution of the DN-BVP on $\mathcal{A}$ which has the same boundary data as g, and the same conductance constants on edges which do not have type I vertices, then $\bar{g}$ and g have the same values on $\mathcal{T}^{(0)}$ and $\bar{g}$ is a linear extension of g at vertices of type I.

Lemma 4.3. *Let $g_2 = \bar{g}|_{\mathcal{A}_{l_s,E_2}}$, the solution of the D-BVP defined on $\mathcal{A}_{l_s,E_2}$, and let $\bar{g}_1 = g|_{\mathcal{A}_{l_s,E_2}}$, the solution of the DN-BVP defined on the quadrilateral $\mathcal{A} \setminus (\mathcal{A}_{l_s,E_2})^0$. Then the length of l_s measured with respect to the flux-gradient metric of g_1 is equal to its length measured with respect to the flux-gradient metric of g_2.*

Proof. Since $\bar{g}$ is harmonic at each vertex in $\mathcal{V}$ which is different from u_s, and since the Neumann derivative of g at u_s is zero, we have that

$$\sum_{v_i\in\mathcal{V},\, v\neq u_s} \sum_{y\sim v_i} c(y, v_i)\big(\bar{g}(v_i) - \bar{g}(y)\big) + \frac{\partial \bar{g}}{\partial n}(\mathcal{A})(u_s) = 0. \tag{4.4}$$

We now split the neighbors of each vertex in $\mathcal{V}$ other than u_s into two groups. For each $i = 1, \ldots, k$, let $\mathcal{A}_{l_s,E_2}(v_i) = \{v_i^1, \ldots, v_i^{j(i)}\}$ be the neighbors of v_i which are contained in $(\mathcal{A}_{l_s,E_2})^0$ and let $\mathcal{Q}_{l_s,E_2}(v_i) = \{v_i^{j(i)+1}, \ldots, v_i^{t(i)}\}$ be the rest of its neighbors. Let $\{u_s^1, \ldots, u_s^p\}$ be the neighbors of u_s in $(\mathcal{A}_{l_s,E_2})^0$ and let $\{u_s^{p+1}, \ldots, u_s^q\}$ be the rest of its neighbors. We now rewrite Eq. (4.4) in the following form:

$$\sum_{v_i \in \mathcal{V},\, v \neq u_s} \left(\sum_{y \sim v_i \wedge y \in \mathcal{A}_{l_s,E_2}(v_i)} c(y, v)\big(\bar{g}(v) - \bar{g}(y)\big) + \sum_{y \sim v_i \wedge y \in \mathcal{Q}_{l_s,E_2(v_i)}} c(y, v_i)\big(\bar{g}(v_i) - \bar{g}(y)\big) \right)$$
$$+ \sum_{r=1}^{p} c\big(u_s, u_s^r\big)\big(g(u_s) - g\big(u_s^r\big)\big) + \sum_{w=p+1}^{q} c\big(u_s, u_s^w\big)\big(g(u_s) - g\big(u_s^w\big)\big) = 0. \tag{4.5}$$

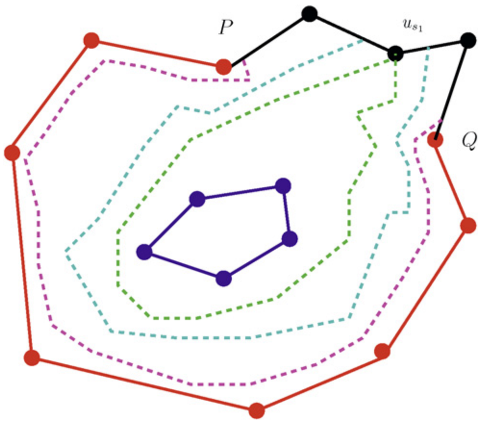

Fig. 4.6. A few level curves in Example 4.2.

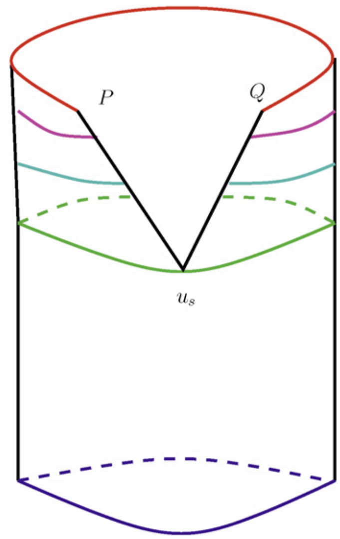

Fig. 4.7. The associated surface.

By the definition of the flux-gradient metric, splitting the sum above into two groups and taking absolute values, the assertion of the lemma follows. □

Example 4.8 *(An annulus with one inner Neumann arc).* The analysis is similar to the one in the previous example. Let $\mathcal{A}$ be a planar annulus with $\partial\mathcal{A} = E_1 \cup E_2$, where E_1 is the outer boundary. Let β_1 be a closed arc in E_2 with endpoints Q and P. We solve the DN-BVP as described in the introduction. In particular, we have $m = 1$ and $t = 4$, and hence that the right-hand side of Eq. (3.12) minus $t/4$ is equal to $-\frac{1}{2}$. Therefore, the only possibility is that there exists only one singular boundary vertex which belongs to $E_2 \setminus \beta_1$. We will denote this vertex by v_s, and its associated level curve by l_s. Since the index of v_s is equal to $-\frac{1}{2}$, there must be at least two arcs of l_s which pass through v_s. It follows by the maximum principle that there are exactly two arcs, and that l_s is simple. Moreover, $E_1 \cup L_s$ comprises the boundary of an annulus which we will denote by $\mathcal{A}_{l_s,E_1}$. It follows that $\mathcal{A}$ is topologically the union (along l_s) of a sliced quadrilateral in which two adjacent vertices have been identified to one, v_s, and an annulus. Arguing in a similar way to Lemma 4.3 shows that this decomposition is geometric. The length of l_s measured with respect to the flux-gradient metric of the induced D-BVP on $\mathcal{A}_{l_s,E_1}$, is the same as measured with respect to the flux-gradient metric of the induced DN-BVP in $\mathcal{Q}_{\mathcal{A}_{l_s,E_2}} = \mathcal{A} \setminus (\mathcal{A}_{l_s,E_1})^0$.

Remark 4.9. The surface associated with this example is basically obtained by turning the previous one upside down.

Example 4.10 *(An annulus with one outer and one inner Neumann arc).* The analysis of this case relies on the results and principles set forth in the preceding two examples. Let $\mathcal{A}$ be a planar annulus with $\partial\mathcal{A} = E_1 \cup E_2$, where E_1 is the outer boundary. Let α_1 be a closed arc in E_1 with endpoints Q and P, and let β_1 be a closed arc in E_2 with endpoints S and T. We solve the DN-BVP as described in the introduction. In particular, we have $l + m = 2$ and $t = 4$, and hence that the right-hand side of Eq. (3.12) minus $t/4$ is equal to -1. By using the local structure of an interior singular vertex of index -1, the maximum principle or the fact that g has different values on the pairs $\{P, Q\}$ and $\{S, T\}$, one can show that an interior singular vertex of index -1 cannot occur. Similarly one rules out the case of a boundary singular vertex of index -1. Hence, the only possible way in which equality may hold in Eq. (3.12) is the case in which there exist two singular boundary vertices, each of index $-\frac{1}{2}$. With some additional work one shows that $E_1 \setminus \alpha_1$ contains one of these, say u_{s_1}, and $E_2 \setminus \beta_1$ contains the other, say u_{s_2}. It follows from the maximum principle that u_{s_1} and u_{s_2} have different g values. In particular, their associated level curves l_{s_1} and l_{s_2} are disjoint. As in the preceding two examples, there are exactly two arcs (of the appropriate level curve) meeting at a singular vertex. Hence, $\mathcal{A}$ is topologically the union of three pieces. The first is a sliced quadrilateral whose boundary consists of E_2 and l_{s_2} which will be denoted by $\mathcal{Q}_{E_2,l_{s_2}}$. The second piece is an annulus whose boundary consists of l_{s_2} and l_{s_1} which will be denoted by $\mathcal{A}_{l_{s_1},l_{s_2}}$. The third piece is a sliced quadrilateral whose boundary consists of l_{s_1} and E_1 which will be denoted by $\mathcal{Q}_{E_1,l_{s_1}}$. We have

$$\mathcal{Q}_{E_2,l_{s_2}} \cap \mathcal{A}_{l_{s_1},l_{s_2}} = l_{s_2} \quad \text{and} \quad \mathcal{Q}_{E_1,l_{s_1}} \cap \mathcal{A}_{l_{s_1},l_{s_2}} = l_{s_1}. \tag{4.11}$$

A simple generalization of Lemma 4.3 shows that the gluing is geometric. That is, for $i = 1, 2$, the length of l_{s_i} measured with respect to the flux-gradient metric by the induced D-BVP on $\mathcal{A}_{l_{s_1},l_{s_2}}$, equals the length measured with respect to the flux-gradient metric by the induced DN-BVP on $\mathcal{Q}_{E_1,l_{s_1}}$ and $\mathcal{Q}_{E_2,l_{s_2}}$, respectively (as before, one needs to add vertices of type I and type II, if necessary).

Remark 4.12. The surface associated with this example is basically the "union" of the surfaces in the previous two.

Example 4.13 *(A planar pair of pants with one outer Neumann arc).* Let $\mathcal{P}$ be a planar pair of pants with $\partial\mathcal{P} = E_1 \cup E_2$, where E_1 is the outer boundary and $E_2 = E_2^1 \sqcup E_2^2$ is the inner boundary. Let α_1 be a closed arc in E_1 with endpoints Q and P. We solve the DN-BVP as described in the introduction. In particular, we have $m = 1$ and $t = 2$, and hence that the right-hand side of Eq. (3.12) minus $t/4$ is equal to $-\frac{3}{2}$. By applying the maximum principle, the case in which there exist three singular vertices each having its index equal to $-\frac{1}{2}$, and the case of two singular boundary vertices, one of which has index -1 and the other has index $-\frac{1}{2}$, can be easily ruled out. We are left with the possibility that there exists one interior singular vertex, u_{s_1}, whose index equals -1 and one boundary singular vertex, u_{s_2}, whose index is equal to $-\frac{1}{2}$. Let l_{s_1} be the singular level curve passing through u_{s_1} and let l_{s_2} the singular level curve passing through u_{s_2}. Arguing as in the previous examples, there are exactly two arcs of the singular curve passing through u_{s_2} and four arcs passing through u_{s_1}.

There are two cases to consider. First assume that u_{s_1} and u_{s_2} have the same g-value (see Figs. 4.14 and 4.15). This implies (by using the maximum principle) that they lie on the same singular level curve, which we will denote by l_s. The second case occurs when u_{s_1} and u_{s_2} have different g-values. In the first case the topological decomposition of $\mathcal{P}$ is the following. The two annuli $\mathcal{A}_{E_2^1,l_s}$ and $\mathcal{A}_{E_2^2,l_s}$ which intersect at u_{s_1} are attached to the sliced quadrilateral $\mathcal{Q}_{l_s,E_1}$ along the union of their boundaries, l_s. Observe that in this case $\mathcal{Q}_{l_s,E_1}$ has one singular boundary arc, l_s, at u_{s_1}.

In the second case (Figs. 4.16 and 4.17) the topological decomposition of $\mathcal{P}$ is the following. The two annuli $\mathcal{A}_{E_2^1,l_{s_1}}$ and $\mathcal{A}_{E_2^2,l_{s_2}}$ which intersect at u_{s_1} are attached to the (singular) annulus $\mathcal{A}_{l_{s_1},l_{s_2}}$ along their common boundary, l_{s_1}; the annulus $\mathcal{A}_{l_{s_1},l_{s_2}}$ is attached to the sliced quadrilateral $\mathcal{Q}_{l_{s_2},E_1}$ via their common boundary l_{s_2}. It can be shown by a generalization of Lemma 4.3, that the gluing is geometric.

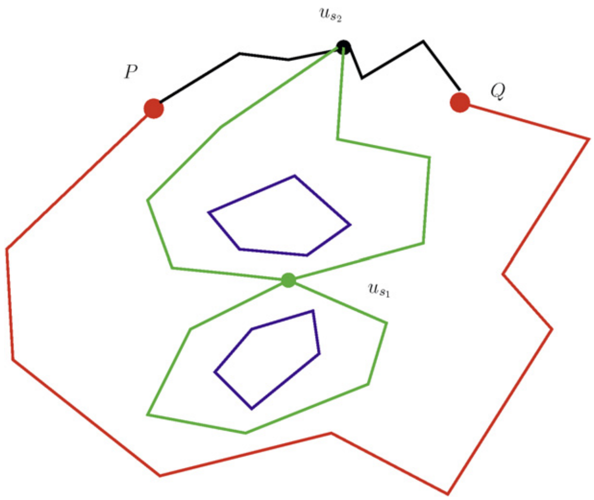

Fig. 4.14. The first case of Example 4.13.

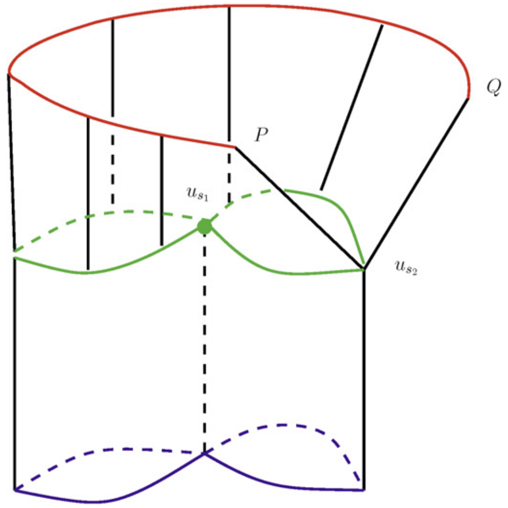

Fig. 4.15. The associated surface.

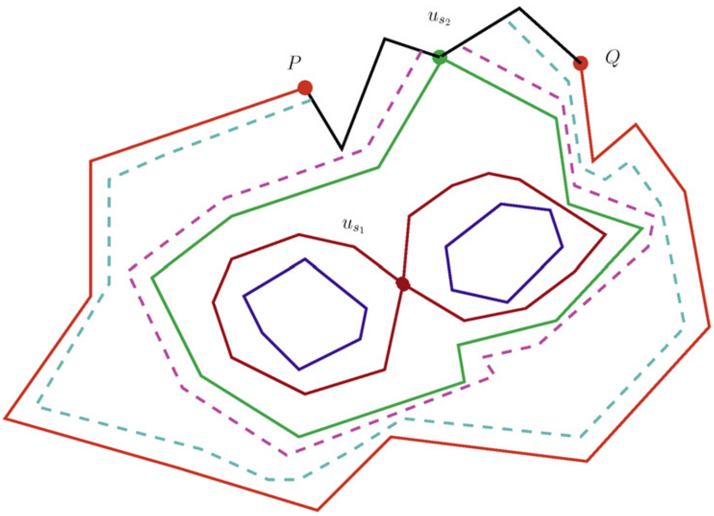

Fig. 4.16. The second case of Example 4.13.

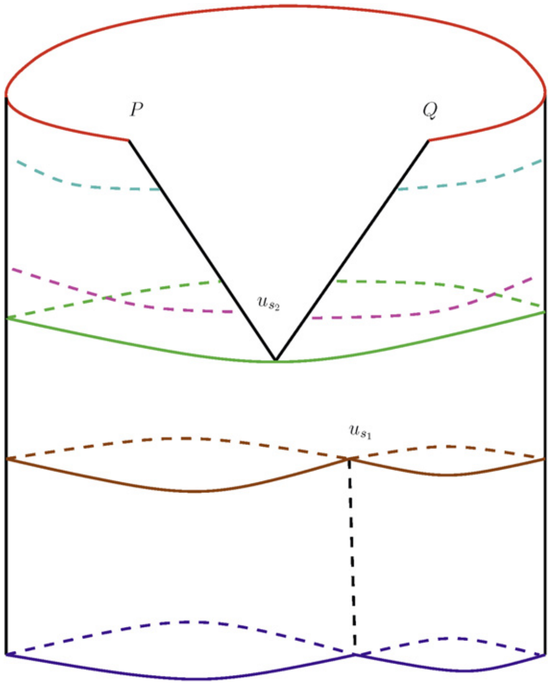

Fig. 4.17. The associated surface.

We finish this section with one more example which illustrates some of the combinatorial complexity of higher genus cases. We will not provide a complete analysis of this case and leave the completion of the details to the reader.

Example 4.18 *(A planar pair of pants with two outer Neumann arcs).* Let $\mathcal{P}$ be a planar pair of pants with its boundary $\mathcal{P} = E_1 \sqcup E_2$, where E_1 is the outer boundary and where $E_2 = E_2^1 \sqcup E_2^2$ is the inner boundary. Let α_1 be a closed arc in E_1 with endpoints P_1 and Q_1 and let α_2 be another closed arc in E_1 with endpoints P_2 and Q_2, respectively; further assume that P_1, Q_1, P_2 and Q_2 are ordered counterclockwise. We solve the DN-BVP as described in the introduction. In particular, we have $l = 2$ and $t = 4$, and hence that the right-hand side of Eq. (3.12) minus $t/4$ is equal to -2. There are several cases in which two boundary vertices, the index of each is equal to $-\frac{1}{2}$, and an interior singular vertex of index which is equal to -1 may occur, and we will now describe two of these.

Let $u_{s_1} \in Q_1P_2$ and $u_{s_2} \in Q_2P_1$ be the two singular boundary vertices and let u_b be the interior singular boundary vertex. First assume that u_{s_1} and u_{s_2} attain the same g values and belong to the same level curve, which is different from the g value attained at u_b (see Fig. 4.19). It follows that l_s, this singular level curve, is a closed (piecewise linear) curve.

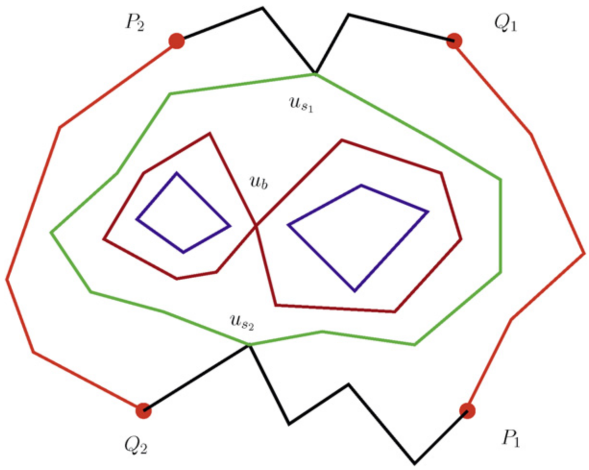

Fig. 4.19. The first case of Example 4.18.

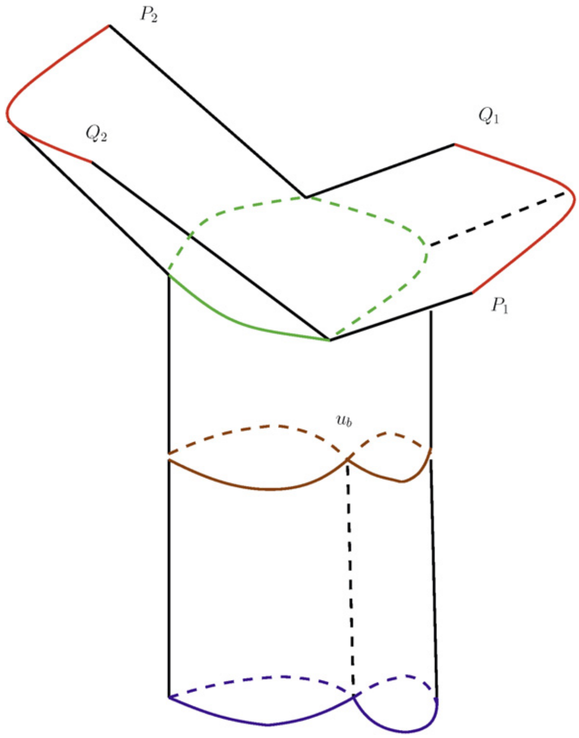

Fig. 4.20. The associated surface.

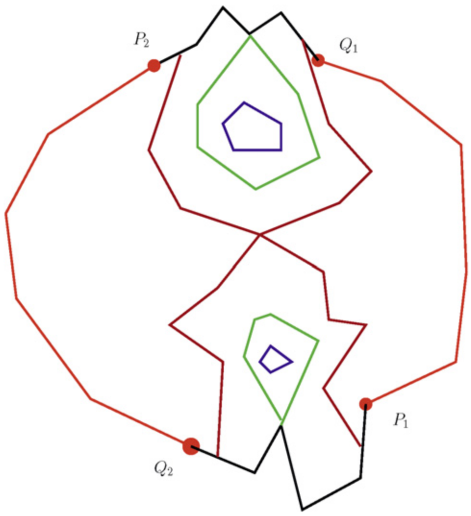

Fig. 4.21. The second case of Example 4.18.

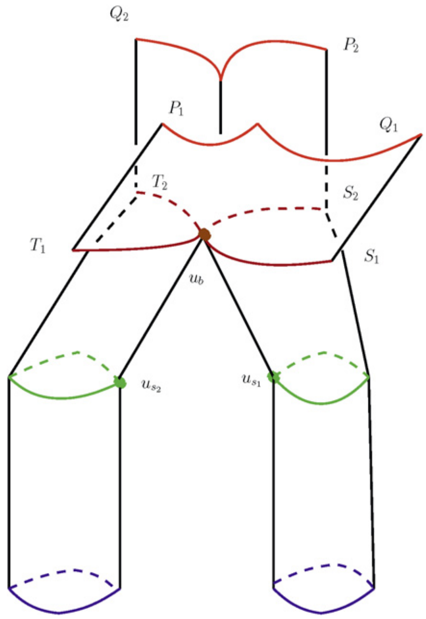

Fig. 4.22. The associated surface.

It follows by the maximum principle that E_2 is contained in the domain bounded by l_s. Also, l_b, the singular level curve which passes through u_b is a piecewise figure eight curve, and (necessarily) the g-value of u_b is smaller than that of the g-value of u_{s_1}. Hence, in this case $\mathcal{P}$ has the following topological decomposition. A quadrilateral $\mathcal{Q}_{\text{right}}$ which has u_{s_1}, Q_1, P_1 and u_{s_2} as its corners. A quadrilateral $\mathcal{Q}_{\text{left}}$ which has u_{s_1}, P_2, Q_2 and u_{s_2} as its corners. A singular annulus $\mathcal{A}_{l_s,l_b}$ with its singular boundary curve being l_b, the other boundary curve being l_s. The singular annulus $\mathcal{A}_{l_s,l_b}$ is attached to $\mathcal{Q}_{\text{right}}$ along the right arc of l_s, the one which connects u_{s_1} to u_{s_2}, and to $\mathcal{Q}_{\text{right}}$ along the left arc of l_s which connects u_{s_1} to u_{s_2} (see Fig. 4.20).

The singular curve $l_b = l_{\text{left}} \cup u_b \cup l_{\text{right}}$ bounds two annuli, $\mathcal{A}_{E_2^1, l_{\text{left}}}$ which has as its boundary E_2^1 and $u_b \cup l_{\text{left}}$, and $\mathcal{A}_{E_2^2, l_{\text{right}}}$ which has as its boundary E_2^2 and $u_b \cup l_{\text{right}}$. These two annuli intersect (only) at the vertex u_b.

We now handle the case in which u_{s_1} and u_{s_2} have the same g-values but belong to different level curves (see Fig. 4.21). Let l_{s_1} be the singular level curve passing through u_{s_1}, and let l_{s_2} the singular level curve passing through u_{s_2}. It is easy to check that l_b must intersect Q_1P_2 in two points which we will denote by S_1 and S_2, respectively, with S_1 between u_{s_1} and Q_1 and with S_2 between u_{s_1} and P_2. Similarly, let T_1 be the intersection point of l_b with Q_2P_1 which is between u_{s_2} and P_1, and let T_2 be the intersection point of l_b with Q_2P_1 which is between u_{s_2} and Q_2. Also, l_{s_1} is simple and closed, $l_{s_1} \cap P_2Q_1 = \{u_{s_1}\}$, and the region it bounds contains E_2^1. Symmetrically, l_{s_2} is simple and closed, $l_{s_2} \cap Q_2P_1 = \{u_{s_2}\}$, and the region it bounds contains E_2^2.

In this case (see Fig. 4.22), the topological decomposition of $\mathcal{P}$ is the following. A quadrilateral $\mathcal{Q}_{\text{left}}$ which has S_2, P_2, Q_2 and T_2 as its corners. A quadrilateral $\mathcal{Q}_{\text{right}}$ which has S_1, Q_1, P_1 and T_1 as its corners. A sliced quadrilateral $\mathcal{Q}_{\text{top}}$ which has S_2, S_1 and u_{s_1} as its corners; it is attached to $\mathcal{Q}_{\text{left}}$ along the arc of l_b determined by S_2 and u_b, and to $\mathcal{Q}_{\text{right}}$ along the arc of l_b determined by S_1 and u_b. A sliced quadrilateral $\mathcal{Q}_{\text{bottom}}$ which has T_1, T_2 and u_{s_2} as its corners; it is attached to $\mathcal{Q}_{\text{left}}$ along the arc of l_b connecting T_2 and u_b, and to $\mathcal{Q}_{\text{right}}$ along the arc of l_b connecting T_1 and u_b. The last two pieces are two annuli, $\mathcal{A}_{E_2^1, l_{s_1}}$ and $\mathcal{A}_{E_2^2, l_{s_2}}$ that are attached to the above sliced quadrilaterals along l_{s_1} and l_{s_2}, respectively. The two sliced quadrilaterals intersects (only) at the vertex u_b. As before, an extension of Lemma 4.3 shows that in both cases the gluing is geometric.

5. The general case – an m-connected bounded planar region, $m > 2$

Proof of Theorem 0.2. Let $\{0, p_1, p_2, \ldots, p_{n-1}, k\}$ be the set of values of g at the singular vertices arranged in an increasing order. We first construct a topological decomposition of Ω. For $i = 0, \ldots, k$, consider the sub-domain of Ω defined by

$$\Omega_i = \left\{ x \in \Omega \;\middle|\; p_i < g(x) < p_{i+1} \right\} \tag{5.1}$$

(where the value at x which is not a vertex is defined by the affine extension of g). In general Ω_i is multi-connected and (by definition) contains no singular vertices in its interior. Let $g_i = g|_{\Omega_i}$ be the restriction of g to $\Omega_i \cup \partial\Omega_i$. The definition of g_i involves (as in the proof of Theorem 0.6) introducing new vertices (of type I and type II), and new edges and their conductance constants. In particular, each g_i is the solution of a D-BVP or a DN-BVP, on each one of the components of Ω_i.

By applying Eq. (3.12) in the proof of Lemma 3.7 to g_i and each component of Ω_i whose boundary is a Jordan curve which contains no singular vertices, we obtain that there are two cases to consider. First, a component of Ω_i is simply connected and therefore $m = 1$ and $t = 4$, hence it is a quadrilateral. Second, a component of Ω_i is not simply-connected. In this case we must have $m = 2$ and $t = 0$, hence this component must be an annulus.

We now treat the remaining cases. First assume that the boundary of a component Ω_i^{Jordan} of Ω_i is a Jordan curve and contains at least one singular vertex which we will denote by v_s. It follows that the value of g at v_s is either p_i or p_{i+1}, and that it does not belong to $\alpha_1 \cup \cdots \cup \alpha_l \cup (E_2 \setminus (\beta_1 \cup \cdots \cup \beta_m))$.

According to the index of $v_s \in \Omega$ with respect to g, we now replace a small neighborhood of v_s in Ω by several disjoint piecewise linear wedges. Each wedge has a copy of v_s as a single vertex, and two consecutive arcs of the associated singular

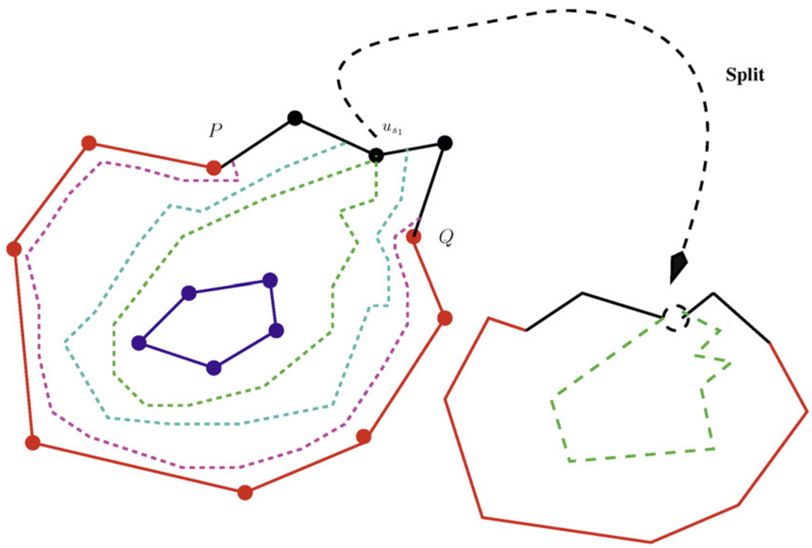

Fig. 5.2. Splitting at u_{s_1}.

level curve, that are contained in the neighborhood, meeting at v_s. If $v_s \in \partial\Omega$, then the only difference from the above, is that exactly two of the wedges will contain as one their arcs part of $\partial\Omega$.

It follows that after finitely many steps (see Fig. 5.2), the boundary of Ω_i^{Jordan} is turned into a Jordan domain with no singular vertices on it. Hence Lemma 3.7 may be applied to the induced Jordan domain and allows us to deduce that Ω_i^{Jordan} is either an annulus or a quadrilateral. It now follows that before the splitting at the singular vertices occurred, Ω_i^{Jordan} was either a quadrilateral in which two adjacent vertices have been identified or an annulus. One should note that singular vertices along the level curves are basically "straightened" along this process in such a way that they become non-singular viewed from g_i and Ω_i^{Jordan} with this boundary modified to a Jordan curve.

We must also consider the case in which the boundary of a component fails to be a Jordan curve. As Example 4.2 shows, this may already occur in the case of Ω being an annulus. This case is treated similarly to the previous one we discussed above (see also Fig. 5.2).

Thus, we conclude that we may decompose Ω into a union (with disjoint interiors) of annuli, quadrilaterals or sliced quadrilaterals. We continue the proof by showing that the gluing is geometric, i.e. that with respect to the boundary value problems induced on each of the components, the common boundary has the same length measure with respect to the flux-gradient metric.

Lemma 5.3. *Let L be a connected arc which is contained in $\Gamma_i \cap \Upsilon_j$, where Γ_i is a component of Ω_i and Υ_j is a component of Ω_j, for some i and j. Then, the length of L measured with respect to the flux-gradient metric induced by $g_i|_{\Gamma_i}$ is equal to its length measured with respect to the flux-gradient metric induced by $g_j|_{\Upsilon_j}$.*

Proof. The proof is a direct generalization of Lemma 4.3 and follows by applying the index lemma (Lemma 3.7) to rule out several cases. Hence, we will only give the details in a few cases.

Observe that the cases in which L is a Neumann arc, or contains a Neumann arc are clearly not possible. By applying the index lemma it can be shown that the cases in which, both Γ_i and Υ_j (Figs. 5.4 and 5.5) are both quadrilaterals is not possible unless L is, without loss of generality, the right boundary of Γ_i as well as the left boundary of Υ_j (this means that $j = i + 1$). One then uses the fact that the induced D-BVP on $\Gamma_i \cup \Upsilon_{i+1}$ is harmonic on L to deduce the assertion. One treats the case in which both Γ_i and Υ_j are annuli in a similar way; deducing that, without loss of generality, $j = i + 1$, and that the outer boundary component of Γ_i is equal to the boundary component of Υ_{i+1} which corresponds to the g value $i + 1$. Again, one uses the harmonicity of the induced D-BVP solution (defined on $\Gamma_i \cup \Upsilon_j$) on L to obtain the assertion.

Assume that (without loss of generality) Γ_i is a quadrilateral and that Υ_j is an annulus. Assume that L is contained in the component of $\partial\Upsilon_j$, denoted by $\partial\Upsilon_j^{p_{i+1}}$, which corresponds to the g value p_{i+1}. Let $\partial\Upsilon_j^{p_i}$ be the second component of Υ_j (which corresponds to the g-value p_i), and let $L_{i+1}^j = \partial\Upsilon_j^{p_{i+1}} \setminus L$. Let P and Q be the endpoints of L. Assume that P and Q correspond to the g value p_{i+1} and are singular vertices. Since L must lie on $\partial\Upsilon_j$, it follows that the domain bounded by $\Gamma_i \cup \Upsilon_j \setminus L$ is an annulus. However, since in this case $t = 2$, we much have (by the index lemma) a boundary singular vertex, this is absurd.

We now treat one case in which the index lemma does not provide an obstruction for an intersection (see Section 4 for more). The setting is as in the above case, with Γ_i being this time a sliced quadrilateral. Let A, C, D, B be the vertices of Γ_i arranged clockwise and let A, B be the vertices which are identified. The value of g_i on the arc AB is p_{i+1}.

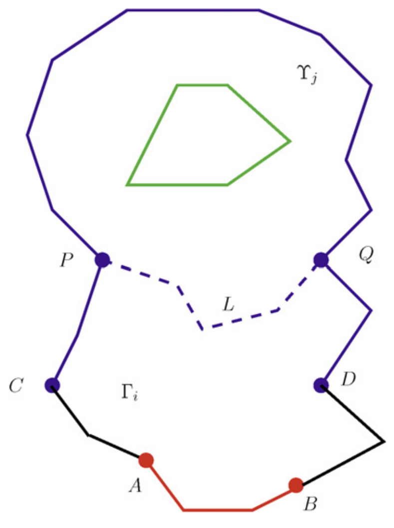

Fig. 5.4. Viewing Γ_i and Υ_j.

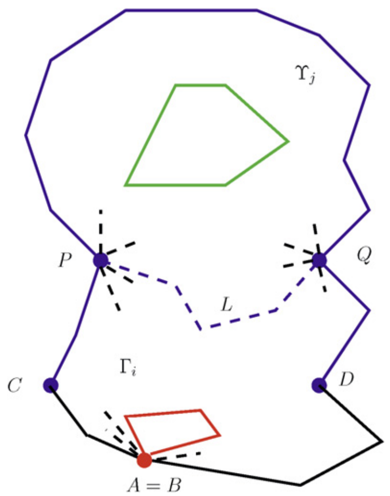

Fig. 5.5. Viewing Γ_i and Υ_j.

We need to prove that

$$\sum_{x\in L}\frac{\partial g_i}{\partial n}(\Gamma_i)(x)+\sum_{x\in L}\frac{\partial g_j}{\partial n}(\Upsilon_j)(x)=0. \tag{5.6}$$

By applying Green's theorem to Γ_i, Υ_j and $\Gamma_i\cup\Upsilon_j$, respectively, we obtain the following equations:

$$0=\sum_{x\in BA}\frac{\partial g_i}{\partial n}(\Gamma_i)(x)+\sum_{x\in CP}\frac{\partial g_i}{\partial n}(\Gamma_i)(x)+\sum_{x\in L}\frac{\partial g_i}{\partial n}(\Gamma_i)(x)+\sum_{x\in QD}\frac{\partial g_i}{\partial n}(\Gamma_i)(x), \tag{5.7}$$

$$0=\sum_{x\in\partial\Upsilon_j^{p_i}}\frac{\partial g_j}{\partial n}(\Upsilon_j)(x)+\sum_{x\in L_{i+1}^j}\frac{\partial g_j}{\partial n}(\Upsilon_j)(x)+\sum_{x\in L}\frac{\partial g_j}{\partial n}(\Upsilon_j)(x), \tag{5.8}$$

$$0=\sum_{x\in BA}\frac{\partial g_i}{\partial n}(\Gamma_i)(x)+\sum_{x\in CP}\frac{\partial g_i}{\partial n}(\Gamma_i)(x)+\sum_{x\in L_{i+1}^j}\frac{\partial g_j}{\partial n}(\Upsilon_j)(x)+\sum_{x\in QD}\frac{\partial g_i}{\partial n}(\Gamma_i)(x)+\sum_{x\in\partial\Upsilon_j^{p_i}}\frac{\partial g_j}{\partial n}(\Upsilon_j)(x). \tag{5.9}$$

By subtracting the third equation from the first and adding the second equation, Eq. (5.6) follows. One verifies by using the method above, that other (finitely many) possible cases, lead as well to assertion of the lemma. □

We now successively apply the assertions of Theorems 0.6 and 0.4 to the appropriate components of Ω. One needs only observe that the tilling thus obtained is consistent as defined in the discussion preceding Proposition 2.17 (see also [16]). This follows by a straightforward generalization of the arguments given in the proof of Proposition 2.17 (see the proof of Theorem 0.4 and the proofs of [16, Theorem 0.1, Theorem 0.4]). □

Remark 5.10. The analysis of the cone singularities is almost identical to the one carried in [16, Section 4.2]. One observes the following additional cases. The presence of propellors results in the creation of new cone singularities of angle $\pi/2$ at each vertex. Hence, under the doubling, if such vertex belongs to a unique propellor, the cone angle will change to π (see for instance vertices P_1, Q_1, P_2, Q_2 in Example 4.18). A similar analysis holds if such a vertex belongs to two rectangles and a non-singular component of a Euclidean cylinder (yielding a cone angle of 4π in the double). Finally, at the singular vertex of a sliced rectangle the cone angle is π, and the analysis of the changes of this angle under doubling is easy to carry (see for instance vertex v_s in Example 4.2).

Remark 5.11. There is a technical difficulty in our construction if some pair of adjacent vertices of $\mathcal{T}^{(0)}$ has the same g-value (the first occurrence is in Eq. (3.1)). One may generalize the definitions and the index formula to allow rectangles of area zero, as one solution. For a discussion of this approach and others see [19, Section 5]. Experimental evidence shows that when the cell decomposition is complicated enough, even when the conductance function is identically equal to 1 and the cells are triangles, such equality rarely happens (for D-BVP).

Remark 5.12. The existence of singular curves for g results in the fact that some rectangles are not embedded in the target. This is evident by Remark 2.24 and the proof of Theorem 0.2. Since some of the cylinders or sliced quadrilaterals constructed have a singular boundary component, it is clear that some points in different rectangles that lie on this level curve will map to the same point. However, this occurs only in the situation described above, and since this fact is not of essential interest to us, we will not go into more details.

Acknowledgements

Some of the results of this paper (as well as from [16]) were presented at the G^3 (New Orleans, January 2007), the Workshop on Ergodic Theory and Geometry (Manchester Institute for Mathematical Sciences, April 2008), the conference "Around Cannon's Conjectur" (Autrans-France, April 2010), and the FRG conference on low dimensional geometric topology (Princeton, March 2011). We deeply thank the organizers for the invitations and well-organized conferences.

References

[1] L.V. Ahlfors, Conformal Invariants – Topics in Geometric Function Theory, McGraw–Hill Book Company, 1973.
[2] T. Banchoff, Critical points and curvature for embedded polyhedra, J. Differential Geometry 1 (1967) 245–256.
[3] E. Bendito, A. Carmona, A.M. Encinas, Solving boundary value problems on networks using equilibrium measures, J. Func. Analysis 171 (2000) 155–176.
[4] E. Bendito, A. Carmona, A.M. Encinas, Shortest paths in distance-regular graphs, Eur. J. Combinatorics 21 (2000) 153–166.
[5] E. Bendito, A. Carmona, A.M. Encinas, Equilibrium measure, Poisson kernel and effective resistance on networks, in: V. Kaimanovich, K. Schmidt, W. Woess (Eds.), Proceedings in Mathematics, vol. 174, De Gruyter, 2003, pp. 363–376.
[6] E. Bendito, A. Carmona, A.M. Encinas, Difference schemes on uniform grids performed by general discrete operators, Applied Numerical Mathematics 50 (2004) 343–370.

[7] I. Benjamini, O. Schramm, Random walks and harmonic functions on infinite planar graphs using square tilings, Ann. Probab. 24 (1996) 1219–1238.
[8] R.L. Brooks, C.A. Smith, A.B. Stone, W.T. Tutte, The dissection of squares into squares, Duke Math. J. 7 (1940) 312–340.
[9] J.W. Cannon, The combinatorial Riemann mapping theorem, Acta Math. 173 (1994) 155–234.
[10] J.W. Cannon, W.J. Floyd, W.R. Parry, Squaring rectangles: the finite Riemann mapping theorem, in: Contemporary Mathematics, vol. 169, Amer. Math. Soc., Providence, 1994, pp. 133–212.
[11] F.R. Chung, A. Grigoŕyan, S.T. Yau, Upper bounds for eigenvalues of the discrete and continuous Laplace operators, Adv. Math. 117 (1996) 165–178.
[12] M. Dehn, Zerlegung von Rechtecke in Rechtecken, Mathematische Annalen 57 (1903) 144–167.
[13] R. Duffin, The extremal length of a network, J. Math. Anal. Appl. 5 (1962) 200–215.
[14] B. Fuglede, On the theory of potentials in locally compact spaces, Acta Math. 103 (1960) 139–215.
[15] S. Hersonsky, Energy and length in a topological planar quadrilateral, Eur. J. Combinatorics 29 (2008) 208–217.
[16] S. Hersonsky, Boundary value problems on planar graphs and flat surfaces with integer cone singularities I: The Dirichlet problem, Crelle, accepted for publication, November 2010.
[17] S. Hersonsky, Boundary value problems on planar graphs and flat surfaces with integer cone singularities III, in preparation.
[18] P. Hubert, H. Masur, T. Schmidt, A. Zorich, Problems on billiards, flat surfaces and translation surfaces, in: Problems on Mapping Class Groups and Related Topics, in: Proc. Sympos. Pure Math., vol. 74, Amer. Math. Soc., Providence, RI, 2006, pp. 233–243.
[19] R. Kenyon, Tilings and discrete Dirichlet problems, Israel J. Math. 105 (1998) 61–84.
[20] F. Lazarus, A. Verroust, Level set diagrams of polyhedral objects, in: Proceedings of ACM Symposium on Solid and Physical Modeling, Ann Arbor, Michigan, ACM Press, 1999, pp. 130–140.
[21] H. Masur, Ergodic theory of translation surfaces, in: Handbook of Dynamical Systems, vol. 1B, Elsevier, Amsterdam, 2006, pp. 527–547.
[22] O. Schramm, Square tilings with prescribed combinatorics, Israel J. Math. 84 (1993) 97–118.
[23] P.M. Soardi, Potential Theory on Infinite Networks, Lecture Notes in Mathematics, vol. 1590, Springer-Verlag, Berlin–Heidelberg, 1994.
[24] A. Zorich, Flat surfaces, in: Frontiers in Number Theory, Physics, and Geometry, I, Springer, Berlin, 2006, pp. 437–583.